FERMILAB-PUB-08-555-E

Radiation Damage Studies of Silicon Photomultipliers

P. Bohn, A. Clough, E. Hazen, A. Heering, and J. Rohlf

Department of Physics, Boston University, Boston, MA 02212, USA

J. Freeman and S. Los

Fermi National Accelerator Laboratory, Batavia, IL 60510, USA

E. Cascio

Francis H. Burr Proton Therapy Center, Massachusetts General Hospital, Boston, MA 02114

S. Kuleshov [1]

Institute for Theoretical and Experimental Physics, Moscow, Russia

Y. Musienko [2]

Department of Physics, Northeastern University, Boston, MA 02115, USA

C. Piemonte

Fondazione Bruno Kessler, Trento, I-38050, Italy

[1] Also at Departamento de Fisica y Centro de Estudios Subatomicos, Universidad Tecnica Federico Santa Maria, Casilla 110-V, Valparaiso, Chile

[2] On leave from INR, Moscow, Russia

Abstract

We report on the measurement of the radiation hardness of silicon photomultipliers (SiPMs) manufactured by Fondazione Bruno Kessler in Italy (1 mm^2 and 6.2 mm^2), Center of Perspective Technology and Apparatus in Russia (1 mm^2 and 4.4 mm^2), and Hamamatsu Corporation in Japan (1 mm^2). The SiPMs were irradiated using a beam of 212 MeV protons at Massachusetts General Hospital, receiving fluences of up to 3×10^{10} protons per cm^2 with the SiPMs at operating voltage. Leakage currents were read continuously during the irradiation. The delivery of the protons was paused periodically to record scope traces in response to calibrated light pulses to monitor the gains, photon detection efficiencies, and dark counts of the SiPMs. The leakage current and dark noise are found to increase with fluence. Te leakage current is found to be proportional to the mean square deviation of the noise distribution, indicating the dark counts are due to increased random individual pixel activation, while SiPMs remain fully functional as photon detectors. The SiPMs are found to anneal at room temperature with a reduction in the leakage current by a factor of 2 in about 100 days.

Keywords: Silicon PM, SiPM, MRS, APD, HPD, Photodetector

PACS Numbers: 29.40.Mc, 29.40.Vj, 29.90.+r

Please send proofs to:
James W. Rohlf
Physics Department
Boston University
Boston, MA, USA
tel.: +1617-353-2600, fax: +1617-353-9393, email: rohlf@bu.edu

1 Introduction

During the last several years, we have investigated the use of silicon photomultipliers (SiPMs) [1]-[2] to collect light from bundles of 1 mm fibers optically connected to the scintillators of the hadron calorimeter of the Compact Muon Solenoid (CMS) [3] at the Large Hadron Collider (LHC) [4]. The SiPMs developed for use at the LHC must be sufficiently radiation hard to withstand the expected fluence. Damage in silicon detectors depends on the flux, type and energy of the particles. The damage produced by protons depends on

their energy-dependant non-ionizing energy losses (NIEL). For LHC detectors, particle fluxes have been calculated in 1 MeV neutron equivalent fluxes. The damage produced by the 212 MeV protons used for these measurements is about 0.8 of that produced by 1 MeV neutrons [5]. The fluence for one LHC lifetime in the proximity of the CMS hadron outer (HO) photodetectors is expected to be approximately equivalent to 10^{10} per cm^2 [6]-[10]. While many silicon devices have been proven to be robust under LHC fluences [11], no previous measurements are available for the latest generation of SiPMs with an active area (A) of several mm^2.

The SiPMs chosen for irradiation were $A = 6.2$ mm^2 round diodes from Fondazione Bruno Kessler (FBK, formerly ICT-irst) in Italy, and $A = 4.4$ mm^2 square diodes from the Center of Perspective Technology and Apparatus (CPTA) in Russia. We also irradiated $A = 1.0$ mm^2 square diodes from FBK, CPTA, and Hamamatsu Corporation (HC) in Japan. All of the SiPMs have a pixel size of 50 μm $\times$ 50 μm [2]. In addition, we made measurements of a single pixel on an FBK 6.2 mm^2 SiPM.

2 Experimental Setup

The radiation studies were carried out at the proton cyclotron [12] at the Massachusetts General Hospital Francis H. Burr Proton Therapy Center in Boston, MA, USA. The proton kinetic energy at the SiPMs was 212 MeV. The beam spot size was 4 cm diameter, allowing irradiation of three SiPMs simultaneously. The fluence delivered on target was measured directly during irradiation using a thin-foil transmission ion chamber whose response was calibrated to the fluence with a Faraday cup. The SiPMs were mounted in groups of 4 on printed circuit boards. The SiPM boards were mounted in a dark box together with a light-emitting diode (LED) as indicated in fig. 1. The three SiPMs to be irradiated were extended vertically above the circuit boards into the proton beam by their electrical leads. A fourth CPTA 4.4 mm^2 SiPM was mounted on each circuit board out of the radiation area and monitored before, during, and after irradiation as a reference diode. The positioning of the SiPM within the beam profile was checked directly with a photographic film exposure as shown in fig. 2

Figure 3 shows a block diagram of the readout. The nominal operating voltage (V_b) was set individually for each SiPM to be approximately 3 V above turn-on (zero current) for the CPTA and FBK devices using Keithley 6487 power supplies. The gain in this region of V_b was measured to be linear, varying from about 20 fC/PE per V for CPTA 4.4 mm^2 to 200 fC/PE per V for FBK 6.2 mm^2. The resulting leakage current (I_b) per SiPM active area was in the range of 1-2 μA/mm^2. The HC SiPMs have a steeper I_b *vs.* V_b curve and were set to

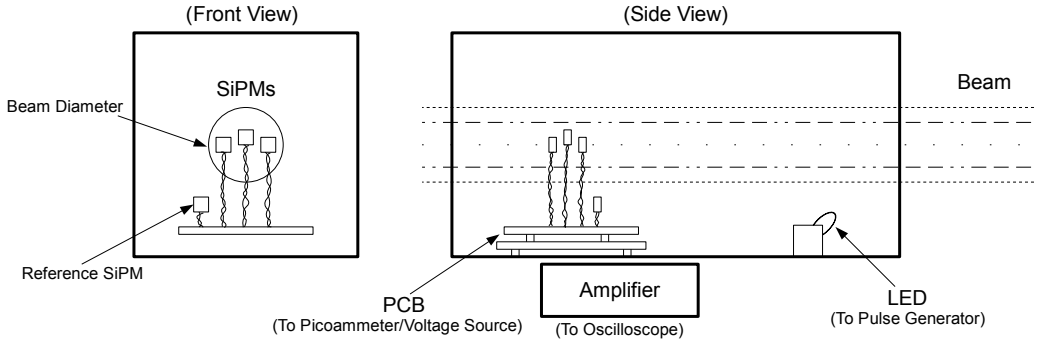

Fig. 1. Layout of the SiPMs in the dark box. Three SiPMs were exposed to protons simultaneously, while a fourth reference SiPM was placed out of the beam. The currents of the SiPMs were read out continuously during exposure. The LED was pulsed before and after the exposure.

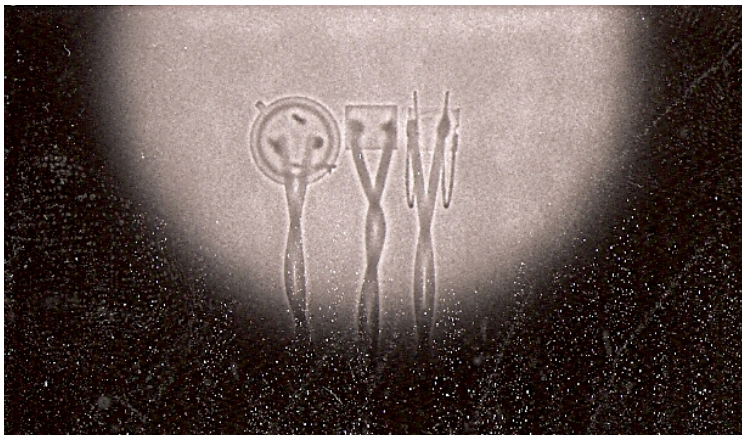

Fig. 2. Exposure of the proton beam to a sheet of polaroid film was used to check positioning of the SiPMs.

be about 1 V above turn-on, resulting in a leakage current per area of about 0.1 μA/mm^2.

The SiPMs were mounted on 4 different circuit boards and were irradiated as summarized in Table 1. Boards 1 and 2 were populated with like SiPMs (CPTA 4.4 mm^2 reference, CPTA 1.0 mm^2, HC 1.0 mm^2, and FBK 1.0 mm^2) and were exposed to fluences of 10^{10} protons per cm^2 for board 1 and 3×10^{10} protons per cm^2 for board 2. Similarly boards 3 and 4 were populated with the same types of SiPMs (CPTA 4.4 mm^2 reference, CPTA 4.4 mm^2, FBK 6.2 mm^2, and FBK single pixel) and irradiated to 10^{10} protons per cm^2 for board 3 and 3×10^{10} protons per cm^2 for board 4. Boards 1 and 3 were irradiated in steps of 2.5×10^9 protons per cm^2 up to a total fluence of 10^{10} protons per cm^2. The fluence for each step was delivered uniformly over a time of 5 minutes. Several minutes were taken between irradiation steps in order to record waveforms. Boards 2 and 4 were irradiated in steps of 2.5×10^9 protons

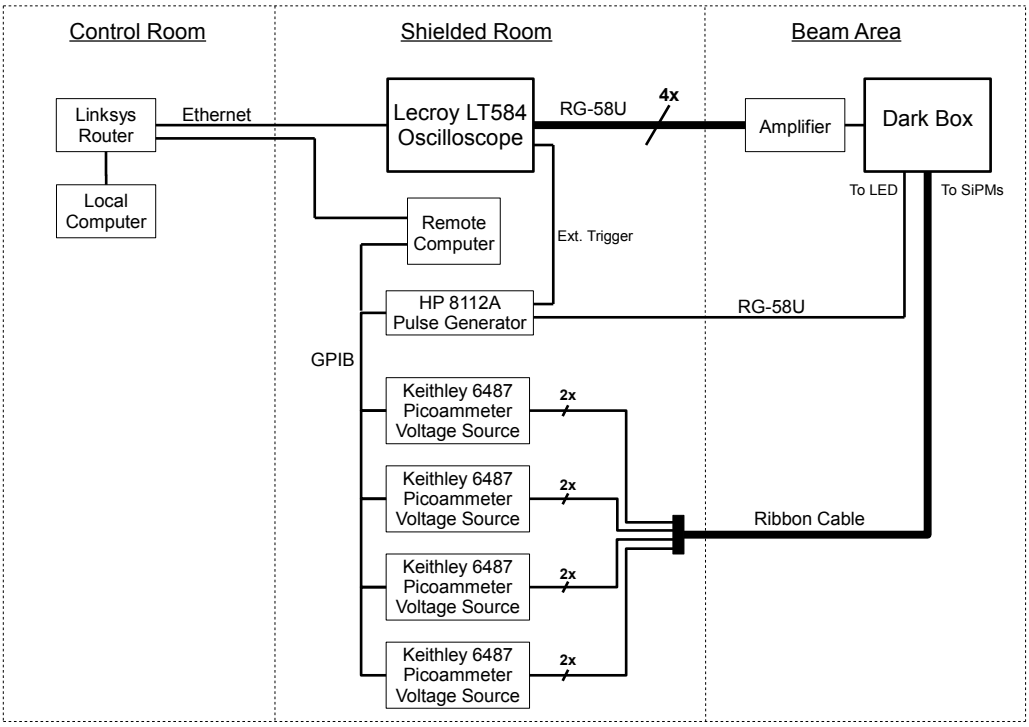

Fig. 3. Layout of the SiPM readout. The digital oscilloscope was viewed and set remotely from the control room out of the radiation zone. The oscilloscope and power supplies were located in a shielded room several meters from the beam area where the SiPMs were mounted in a dark box.

per cm^2 up to a partial fluence of 10^{10} protons per cm^2 and then further exposed with two more steps of 10^{10} protons per cm^2, for a total fluence of 3×10^{10} protons per cm^2. The SiPMs were kept at nominal operating voltage during the irradiation to allow continuous monitoring of $I_{\rm b}$.

The LED was pulsed with a 50 MHz Hewlett-Packard 8112A pulse generator and files of 5000 waveforms were recorded with a Lecroy LT594 digital scope to monitor the pulse shape, signal, and noise distributions. The signal and noise distributions allowed monitoring of the gain (M) and number of photoelectrons ($n_{\rm PE}$). The mean signal (S) in response to the LED may be written as

$$S = M n_{\rm PE} \ ,$$

where the pedestal contribution due to electronic noise has been subtracted. The root mean square (RMS) deviation (σ) from the mean may be written as

$$\sigma = M\sqrt{n_{\rm PE} F} \ ,$$

where the electronic noise has been subtracted in quadrature and F is defined to be the excess noise factor, a number which has been independently measured

Table 1
Irradiated SiPMs, nominal operating voltages, and proton fluences.

Board	*SiPM*	$V_{\rm b}$ (V)	*Fluence* ($\rm cm^{-2}$)
1	CPTA 4.4 $\rm mm^2$ reference	36	0
1	CPTA 1.0 $\rm mm^2$	34	10^{10}
1	HC 1.0 $\rm mm^2$	70.5	10^{10}
1	FBK 1.0 $\rm mm^2$	33.5	10^{10}
2	CPTA 4.4 $\rm mm^2$ reference	35	0
2	CPTA 1.0 $\rm mm^2$	34	3×10^{10}
2	HC 1.0 $\rm mm^2$	70.5	3×10^{10}
2	FBK 1.0 $\rm mm^2$	33.5	3×10^{10}
3	CPTA 4.4 $\rm mm^2$ reference	35	0
3	CPTA 4.4$\rm mm^2$	37	10^{10}
3	FBK 6.2 $\rm mm^2$	34	10^{10}
3	FBK single pixel	37	10^{10}
4	CPTA 4.4 $\rm mm^2$ reference	35	0
4	CPTA 4.4 $\rm mm^2$	37	3×10^{10}
4	FBK 6.2 $\rm mm^2$	34	3×10^{10}
4	FBK single pixel	37	3×10^{10}

to be close to unity for the SiPMs [1]. The measured distribution of S then allows determination of the product of gain times excess noise factor,

$$MF = \frac{\sigma^2}{S} \ ,$$

and the number of photoelectrons divided by the excess noise factor,

$$\frac{n_{\rm PE}}{F} = \frac{S^2}{\sigma^2} \ .$$

3 Leakage Currents During Irradiation

Leakage currents were read continuously during the irradiation. Figure 4 shows $I_{\rm b}/A$ *vs.* time for the SiPMs on board 1. The plateaus correspond to partial fluences of 2.5×10^9, 5×10^9, 7.5×10^9, and 10^{10} protons per $\rm cm^2$, when the

delivery of protons was paused in order to record SiPM waveforms. Figure 5 shows I_b/A *vs.* time for the SiPMs on board 2. The plateaus correspond to partial fluences of 2.5×10^9, 5×10^9, 7.5×10^9, 10^{10}, 2×10^{10}, and 3×10^{10} protons per cm^2. A drop in leakage current due to room-temperature annealing is visible after each irradiation step.

Figure 6 shows I_b/A *vs.* time for the larger-area SiPMs on board 3. The peaks correspond to partial fluences of 2.5×10^9, 5×10^9, 7.5×10^9, and 10^{10} protons per cm^2. A drop in leakage current due to room-temperature annealing is visible after each step and is especially pronounced for the FBK 6.8 mm^2 SiPM. Figure 7 shows I_b/A *vs.* time for the SiPMs on board 4. The peaks correspond to partial fluences of 2.5×10^9, 5×10^9, 7.5×10^9, 10^{10}, 2×10^{10}, and 3×10^{10} protons per cm^2. The leakage currents for the single pixel readouts show a similar time structure with fluence and were in the 50-200 nA range.

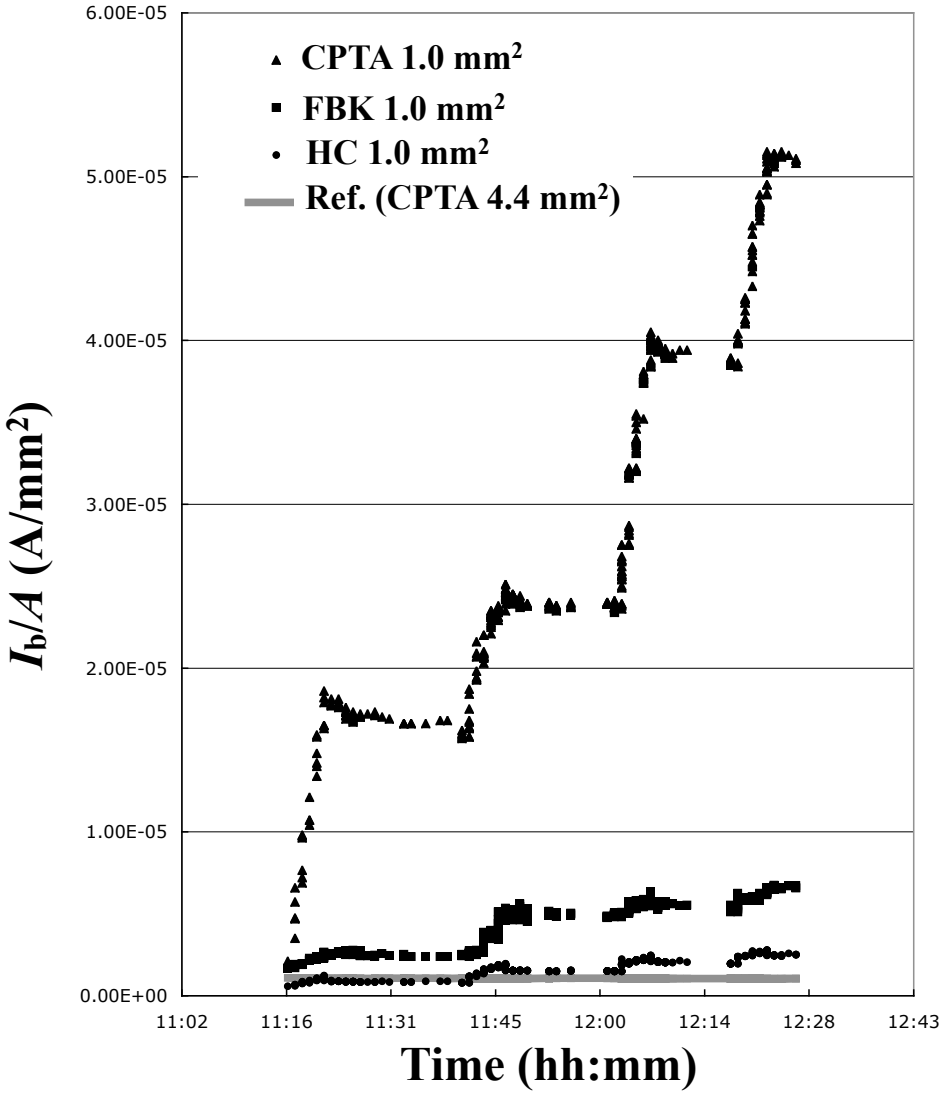

Fig. 4. Leakage currents per area measured during irradiation for SiPMs on board 1: CPTA 4.4 mm^2 reference diode (line), HC 1.0 mm^2 (circles), FBK 1.0 mm^2 (squares), and CPTA 1.0 mm^2 (triangles). The plateaus correspond to partial fluences of 2.5×10^9, 5×10^9, 7.5×10^9, and 10^{10} protons per cm^2. A drop in leakage current due to room-temperature annealing is visible after each step.

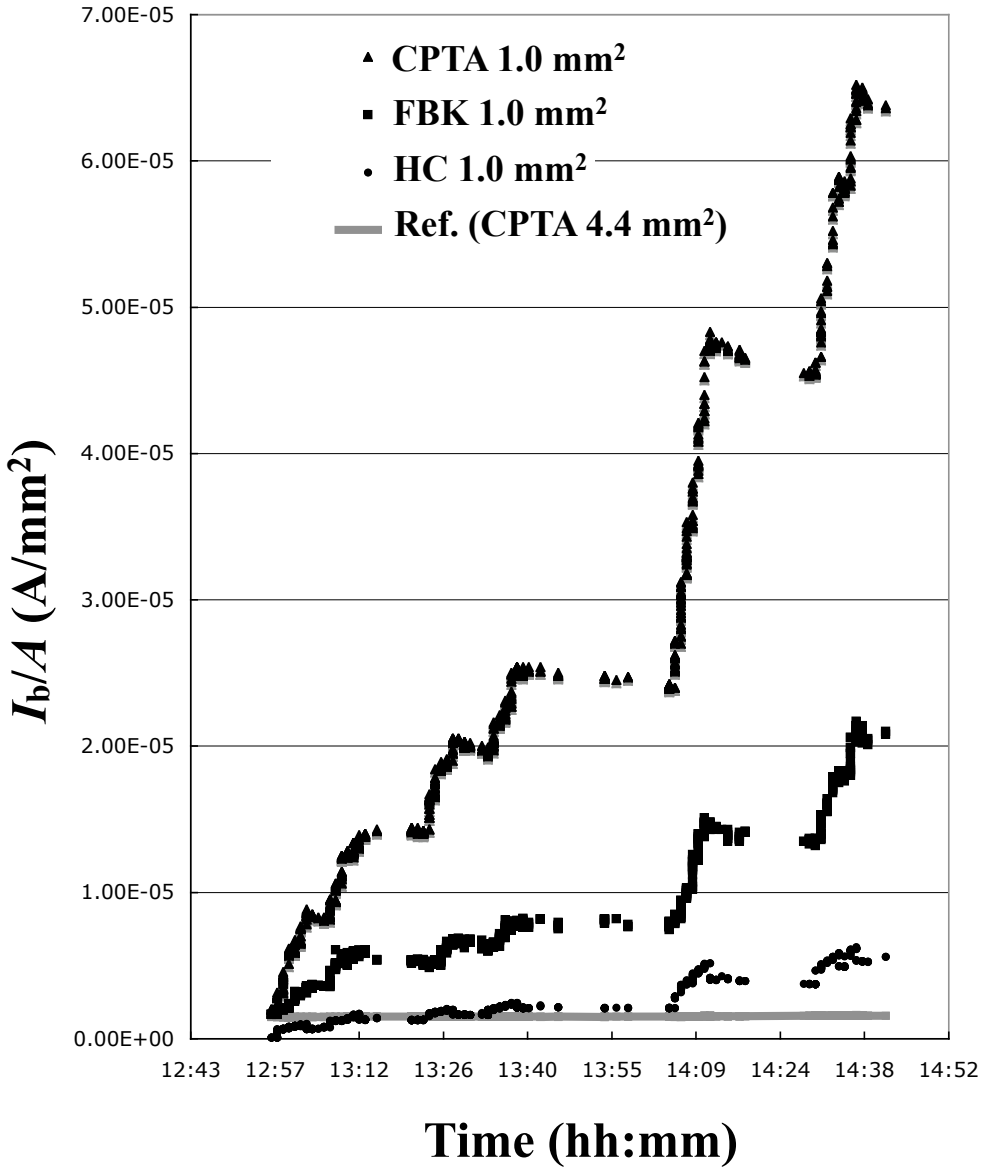

Fig. 5. Leakage currents per area measured during irradiation for SiPMs on board 2: CPTA 4.4 mm^2 reference diode (line), HC 1.0 mm^2 (circles), FBK 1.0 mm^2 (squares), and CPTA 1.0 mm^2 (triangles). The plateaus correspond to partial fluences of 2.5×10^9, 5×10^9, 7.5×10^9, 10^{10}, 2×10^{10}, and 3×10^{10} protons per cm^2. A drop in leakage current due to room-temperature annealing is visible after each step.

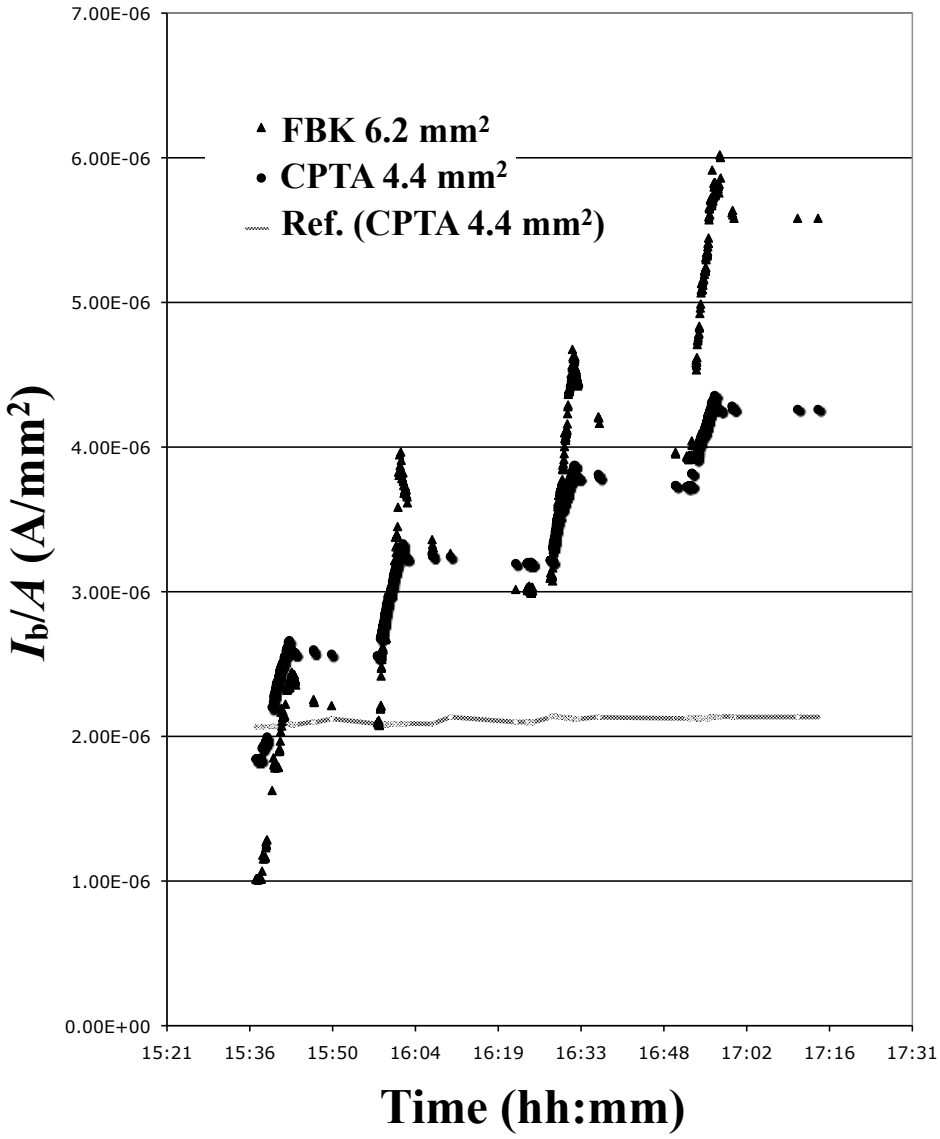

Fig. 6. Leakage currents per area measured during irradiation for SiPMs on board 3: CPTA 4.4 mm^2 reference diode (line), CPTA 4.4 mm^2 (circles), and FBK 6.2 mm^2 (triangles). The plateaus correspond to partial fluences of 2.5×10^9, 5×10^9, 7.5×10^9, and 10^{10} protons per cm^2. A drop in leakage current due to room-temperature annealing is visible after each step.

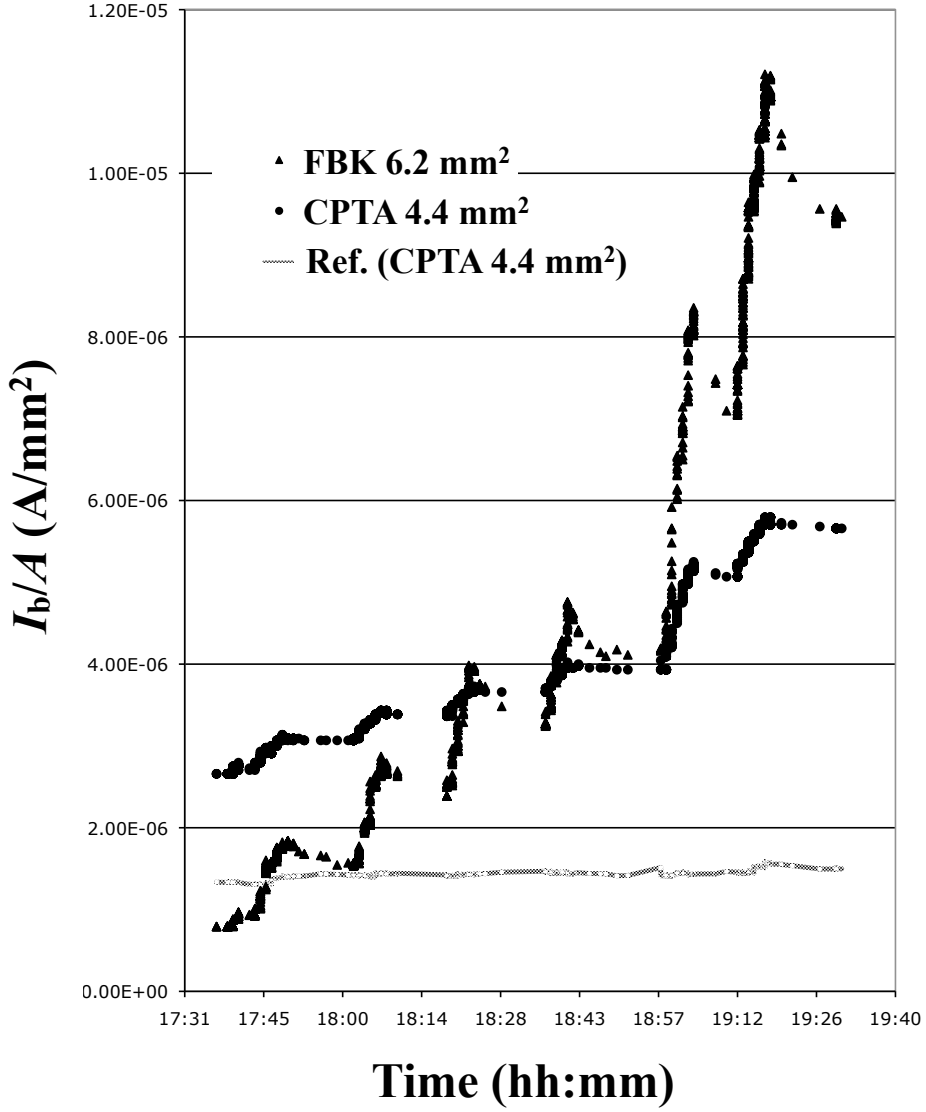

Fig. 7. Leakage currents per area measured during irradiation for SiPMs on board 4: CPTA 4.4 mm^2 reference diode (line), CPTA 4.4 mm^2 (circles), and FBK 6.2 mm^2 (triangles). The plateaus correspond to partial fluences of 2.5×10^9, 5×10^9, 7.5×10^9, 10^{10}, 2×10^{10}, and 3×10^{10} protons per cm^2. A drop in leakage current due to room-temperature annealing is visible after each step.

4 CPTA 4.4 mm^2 Reference SiPMs

A CPTA 4.4 mm^2 SiPM was installed on each board and was not irradiated in order to serve as a reference signal to monitor the stability of the LED. The reference SiPMs were monitored before, during, and after the irradiation. Table 2 shows the currents, gain, number of photoelectrons and signal stability for the reference SiPMs. The data were taken at the same time that the indicated fluence was delivered to the other three SiPMs on each board. There was about an 8 h time difference between the first measurement on board 1 and the last measurement on board 4. The measurements on 15 April 2008 were taken 135 days later. The values of $I_{\rm b}/A$ were stable for all the reference SiPMs. The calculated values of MF from the mean and rms of the LED data were also stable at the few percent level. The values of $n_{\rm PE}/F$ were uniform to a few per cent, indicating that the light output of the LED was relatively stable over this period. A change of the signal response (S) divided by the initial value (S_0) was observed to drift by 5-7% over the measurement period.

5 CPTA 1.0 mm^2

Measurements of $I_{\rm b}$ *vs.* $V_{\rm b}$ were taken before and after each partial fluence. Figure 8 shows $I_{\rm b}$ as a function of $V_{\rm b}$ for CPTA 1.0 mm^2 on board 2 for fluences of zero, 5×10^9, 10^{10}, 2×10^{10}, and 3×10^{10} protons per cm^2. The shape of the $I_{\rm b}$ *vs.* $V_{\rm b}$ distributions indicate that the gain *vs.* voltage is relatively stable. A direct measurement of MF from the mean and width of the response to the LED as a function of voltage before and after irradiation shows that the gain in the region of nominal voltage varies by about 100 fC/PE per V for CPTA 1.0 mm^2 on board 1 and about 50 fC/PE per V for CPTA 1.0 mm^2 on board 2. At a nominal operating voltage of $V_{\rm b} = 34$ V, the leakage current increases from 1.9 μA at zero fluence to 63.6 μA at 3×10^{10} cm^{-2}. Similar $I_{\rm b}$ *vs.* $V_{\rm b}$ curves were observed for the other CPTA 1.0 mm^2 on board 1, where the leakage current at nominal voltage (34 V) increased from 1.5 μA at zero fluence to 51 μA at 10^{10} cm^{-2}.

Table 3 shows the values of $I_{\rm b}$, MF, and $n_{\rm PE}/F$ as defined in section 2, as well as the change in signal S in response to the LED divided by that at zero fluence (S_0). The values of $n_{\rm PE}$ are corrected for the measured deviation of the reference diode (see Table 2). The gain times excess noise factor is observed to decrease from 370 fC/PE to 300 fC/PE for board 1 and from 230 fC/PE to 180 fC/PE for board 2. At large bias currents, a drop in gain is expected due to a reduction in the bias voltage caused by a voltage drop across the 2 kΩ input resistor.

Table 2
Measured properties of the CPTA 4.4 mm^2 reference SiPMs: leakage current, gain, number of photoelectrons, and average response to the LED. The reference SiPMs were not irradiated. The data were taken at the time that the other SiPMs on the same board received the partial fluence indicated in column 2.

Board	*Time*	I_b/A (μA/mm^2)	MF (fC/PE)	n_{PE}/F	S/S_0
1	at zero	1.2	51	146	1
1	at 2.5×10^9 cm^{-2}	1.1	50	148	1.00
1	at 5×10^9 cm^{-2}	1.1	48	150	0.97
1	at 7.5×10^9 cm^{-2}	1.1	50	144	0.96
1	at 10^{10} cm^{-2}	1.1	50	146	0.95
1	15Apr08	1.1	49	141	0.93
2	at zero	1.6	100	170	1
2	at 5×10^9 cm^{-2}	1.6	100	170	0.98
2	at 10^{10} cm^{-2}	1.6	100	170	0.97
2	at 3×10^{10} cm^{-2}	1.8	100	160	0.93
2	15Apr08	1.5	110	150	1.00
3	zero	2.3	110	190	1
3	at 2.5×10^9 cm^{-2}	2.1	100	200	0.94
3	at 5×10^9 cm^{-2}	2.1	100	200	0.95
3	at 7.5×10^{10} cm^{-2}	2.2	100	190	0.95
3	at 10^{10} cm^{-2}	2.1	100	190	0.95
3	15Apr08	2.0	100	200	0.99
4	at zero	1.3	120	140	1
4	at 5×10^9 cm^{-2}	1.4	110	150	0.98
4	at 10^{10} cm^{-2}	1.4	110	140	0.98
4	at 3×10^{10} cm^{-2}	1.5	110	140	0.93
4	15Apr08	1.4	20	140	0.99

The pulse shape in response to the LED was monitored in 500 2 ns time bins. The pulse shape was observed to be stable at all fluences on both boards 1 and 2. Figure 9 shows the average pulse shape on baord 2 summed over 5000 events for a) zero fluence, b) 10^{10} cm^{-2}, and c) 3×10^{10} cm^{-2}. The pulse shape of the CPTA 1.0 mm^2 was observed to have a long time-constant component

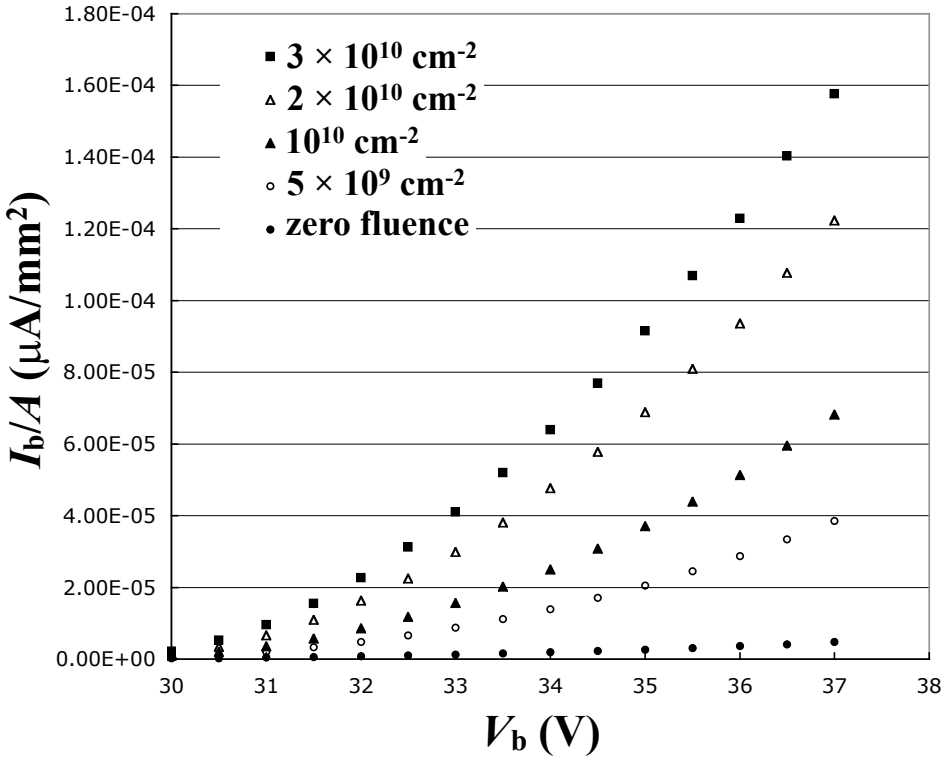

Fig. 8. Leakage currents per mm^2 for CPTA1.0 mm^2 on board 2 as a function of bias voltage for varying proton fluence.

due to a large value of quenching resistance.

The pedestal was summed over 200 ns (bins 1-100 of fig. 9 a),b), and c)) to get the noise distributions in fC shown in fig. 9 for d) zero fluence, e) 10^{10} cm^{-2}, and f) 3×10^{10} cm^{-2} for board 2. The rms noise increases from 192 fC at zero fluence to 670 fC at 10^{10} cm^{-2} to 979 fC at $3{\times}10^{10}$ cm^{-2}. The noise distribution for CPTA 1 mm^2 on board 1 was 277 fC at zero fluence, increasing to 1205 fC at 10^{10} cm^{-2} for $V_{\rm b} = 34$V.

The pulse was summed over 200 ns (bins 151-250 of fig. 9 a),b), and c)) and the pedestal was subtracted to get the signal distributions in fC shown in fig. 9 for g) zero fluence, h) 10^{10} cm^{-2}, and i) 3×10^{10} cm^{-2} for board 2. To calibrate out any instability of the LED, the change in signal was monitored relative to the CPTA 4.4 mm^2 reference SiPM on the same board. The variation of the signals from the reference SIPM varied by 5% for board 1 and 7% for board 2. The signal on the CPTA 1mm^2 SiPM on board 2, relative to zero fluence and corrected for the reference diode signal, was observed to drop by 10% at a fluence of 10^{10} cm^{-2} and 25% at 3×10^{10} cm^{-2}. Similarly, the signal for CPTA 1mm^2 on board 1 was 12% lower at a fluence of 10^{10} cm^{-2}.

Figure 10 shows the square of the rms noise as a function of $I_{\rm b}/A$ for CPTA 1.0 mm^2 on board 2, for data taken immediately after the irradiation (2 Dec 07).

Table 3
Measured properties of the CPTA 1.0 mm^2 SiPMs. The bias voltage was 34 V.

Board	*Fluence* (cm^{-2})	I_b/A (μA/mm^2)	MF (fC/PE)	n_PE/F	S/S_0
1	zero	1.5	370	46	1
1	2.5×10^9	16	330	50	0.96
1	5×10^9	23	340	48	0.96
1	7.5×10^9	39	320	50	0.92
1	10^{10}	51	300	51	0.88
1	15Apr08	30.4	310	51	0.94
2	zero	1.9	230	44	1
2	5×10^9	13.9	220	44	0.94
2	10^{10}	24.7	220	43	0.90
2	3×10^{10}	63.6	180	42	0.75
2	15Apr08	35.8	200	41	0.78

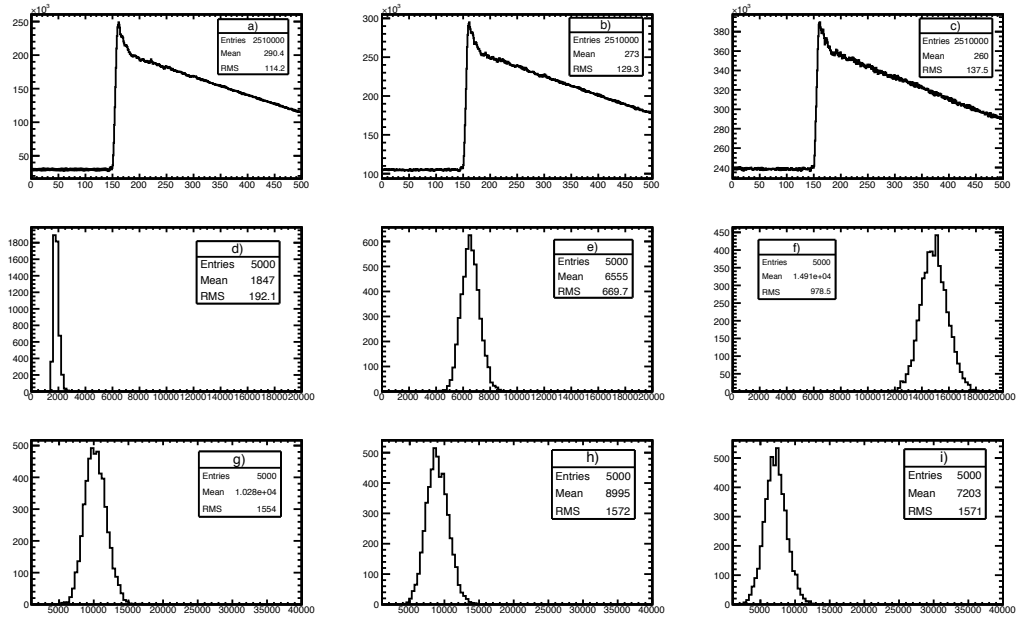

Fig. 9. CPTA1.0 mm^2 at $V_\mathrm{b} = 34$ V on board 2: pulse shape a) before irradiation, b) after 10^{10} cm^{-2}, and c) after 3×10^{10} cm^{-2}; noise distribution d) before irradiation, e) after 10^{10} cm^{-2}, and f) after 3×10^{10} cm^{-2}; and signal distribution in response to LED g) before irradiation, h) after 10^{10} cm^{-2}, and i) after 3×10^{10} cm^{-2}.

The approximate linear dependance indicates that the increase in noise is due to an increase in rate of dark counts, *i.e.* that the leakage current is propor-

tional to the square of the number of activated pixels. Detailed measurements were made after the irradiation as the SiPMs were allowed to anneal at room temperature. A substantal amount of annealing was observed. On 15 Apr 08, 135 days after the irradiation, the dark current had dropped from 63.6 μA to 35.8 μA for CPTA 1.0 mm^2 on board 2. The rms of the noise distribution on 15 Apr 08 was about 4% larger than at the time of irradiation corresponding to the same leakage current as interpolated from the measurements at fluences of 10^{10} cm^{-2} and 2×10^{10} cm^{-2}.

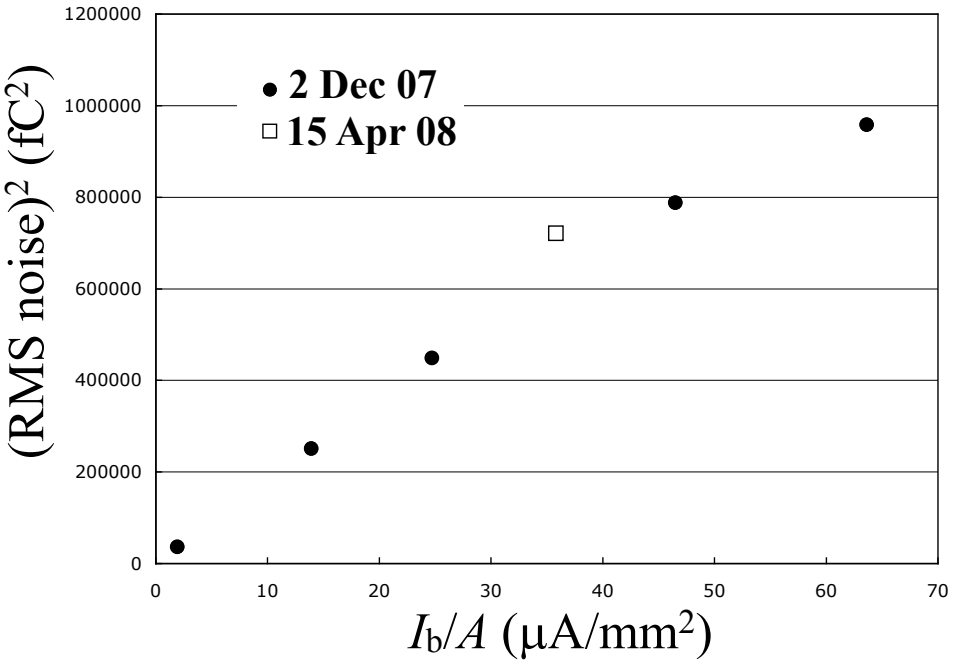

Fig. 10. Pedestal rms noise squared *vs.* leakage current for CPTA 1.0 mm^2 on board 2, for data taken at the time of irradiation, 2 Dec 07 (solid circles) and after room temperature annealing on 15 Apr 08 (open square).

6 HC 1.0 mm^2

Figure 11 shows I_b as a function of V_b for HC 1.0 mm^2 on board 2 for fluences of zero, 5×10^9, 10^{10}, 2×10^{10}, and 3×10^{10} protons per cm^2. The shape of the I_b *vs.* V_b indicate that the gain *vs.* voltage is stable, although the turn-on with voltage is much steeper for the HC 1.0 mm^2 than for the CPTA 1.0 mm^2. A direct measurement of MF as a function of voltage before and after irradiation shows that the gain in the region of nominal voltage varies by about 210 fC/PE per V for HC 1.0 mm^2 on both board 1 and board 2. At a nominal operating voltage of $V_b = 70.5$ V, the leakage current increases from 0.05 μA at zero fluence to 5.6 μA at 3×10^{10} cm^{-2}. Similar I_b *vs.* V_b curves

were observed for the other HC 1.0 mm^2 on board 1, where the leakage current at nominal voltage (70.5 V) increased from 0.1 μA at zero fluence to 2.5 μA at 10^{10} cm^{-2}.

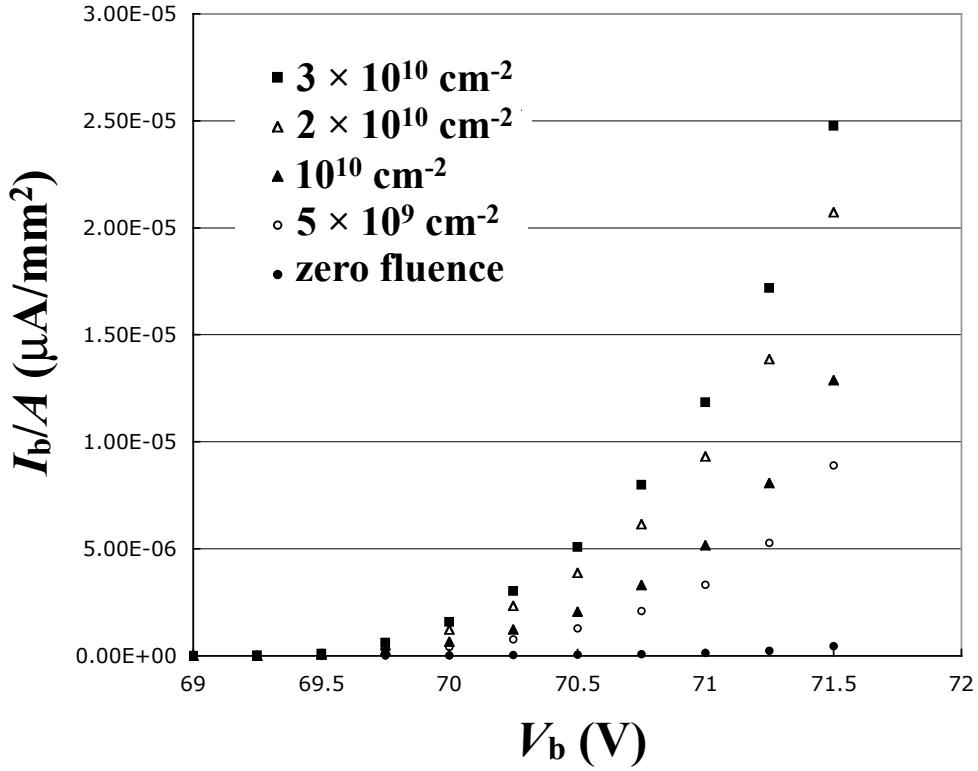

Fig. 11. Leakage currents per mm^2 for HC 1.0 mm^2 on board 2 as a function of bias voltage for varying proton fluence.

Table 4 shows the values of I_b, MF, and n_PE/F and S/S_0. The values of n_PE are again corrected for the measured deviation of the reference diode (see Table 2). The gain times excess noise factor is observed to decrease from 210 fC/PE to 180 fC/PE for board 1 and from 250 fC/PE to 210 fC/PE for board 2. The HC SiPM is especially vulnerable to a drop in gain due to increased bias current because of its sharp turn-on.

The pulse shape for 500 2 ns bins in response to the LED summed over 5000 events is shown in fig. 12 for a) zero fluence, b) 10^{10} cm^{-2}, and c) 3×10^{10} cm^{-2} for board 2. The pulse shape was observed to be stable at all fluences on both boards 1 and 2.

The pedestal was summed over 200 ns (bins 1-100 of fig. 12 a),b), and c)) to get the noise distributions in fC shown in fig. 12 for d) zero fluence, e) 10^{10} cm^{-2}, and f) 3×10^{10} cm^{-2} for board 2. The rms noise increases from 131 fC at zero fluence to 305 fC at 10^{10} cm^{-2} to 436 fC at 3×10^{10} cm^{-2}. The noise distribution for HC 1 mm^2 on board 1 was 126 fC at zero fluence, increasing to 330 fC at 10^{10} cm^{-2} for $V_\mathrm{b} = 70.5$V.

Table 4
Measured properties of the HC 1.0 mm^2 SiPMs. The bias voltage was 70.5 V.

Board	*Fluence* (cm^{-2})	I_b/A (μA/mm^2)	MF (fC/PE)	n_{PE}/F	S/S_0
1	zero	0.1	250	48	1
1	2.5×10^9	0.9	240	47	0.99
1	5×10^9	1.5	230	49	0.94
1	7.5×10^9	2.0	220	50	0.92
1	10^{10}	2.5	210	49	0.89
1	15Apr08	1.1	230	51	1.02
2	zero	0.05	210	48	1
2	5×10^9	1.4	210	47	0.99
2	10^{10}	2.1	200	48	0.94
2	3×10^{10}	5.6	180	47	0.85
2	15Apr08	2.3	210	47	0.98

The signal was summed over 200 ns (bins 151-250 of fig. 12 a),b), and c)) and the noise was subtracted to get the signal distributions in fC shown in fig. 12 for g) zero fluence, h) 10^{10} cm^{-2}, and i) 3×10^{10} cm^{-2} for board 2. The signal on HC 1mm^2 on board 2, relative to zero fluence and corrected for the reference diode signal, was observed to drop by 6% at a fluence of 10^{10} cm^{-2} and 15% at 3×10^{10} cm^{-2}. Similarly, the signal for HC 1mm^2 on board 1 was 11% lower at a fluence of 10^{10} cm^{-2}.

Figure 13 shows the square of the rms noise as a function of I_b/A for HC 1.0 mm^2 on board 2, for data taken immediately after the irradiation (2 Dec 07). The approximate linear dependance indicates that the increase in noise is due to an increase in rate of dark counts, *i.e.* that the leakage current is proportional to the square of the number of activated pixels. Detailed measurements were made after the irradiation as the SiPMs were allowed to anneal at room temperature. A substantial amount of annealing was observed. On 15 Apr 08, 135 days after the irradiation, the dark current had dropped from 5.6 μA to 2.3 μA for HC 1.0 mm^2 on board 2 and from 2.5 μA to 1.1 μA on board 1. The rms of the HC noise distribution on 15 Apr 08 was about 10% larger than that at the time of irradiation corresponding to the same leakage current as interpolated from the measurements at fluences of 10^{10} cm^{-2} and 2×10^{10} cm^{-2}.

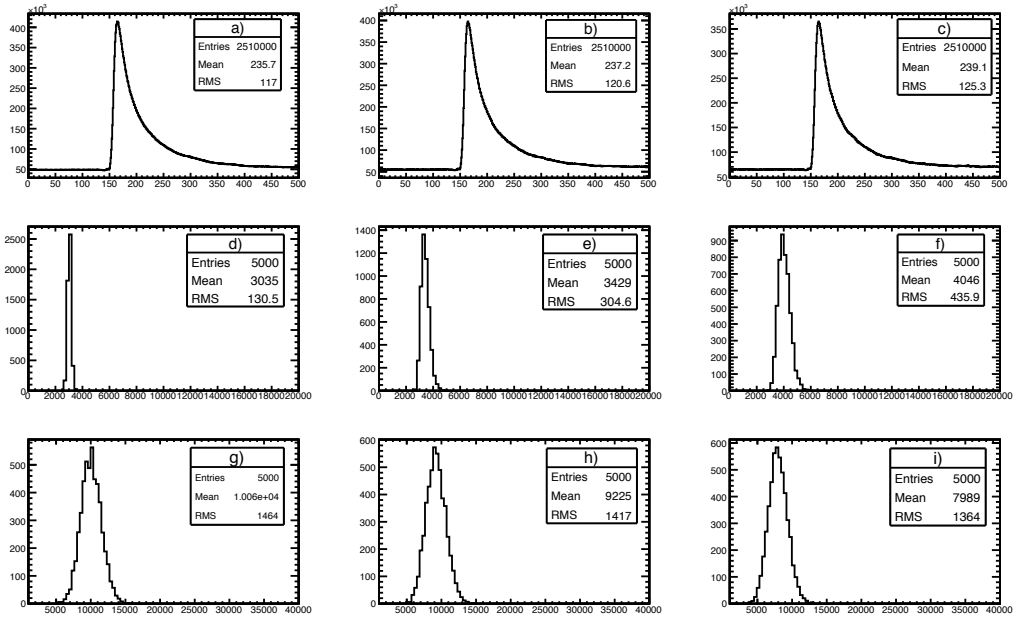

Fig. 12. HC 1.0 mm^2 at $V_\mathrm{b} = 70.5$ V on board 2: pulse shape a) before irradiation, b) after 10^{10} cm^{-2}, and c) after 3×10^{10} cm^{-2}; noise distribution d) before irradiation, e) after 10^{10} cm^{-2}, and f) after 3×10^{10} cm^{-2}; and signal distribution in response to LED g) before irradiation, h) after 10^{10} cm^{-2}, and i) after 3×10^{10} cm^{-2}.

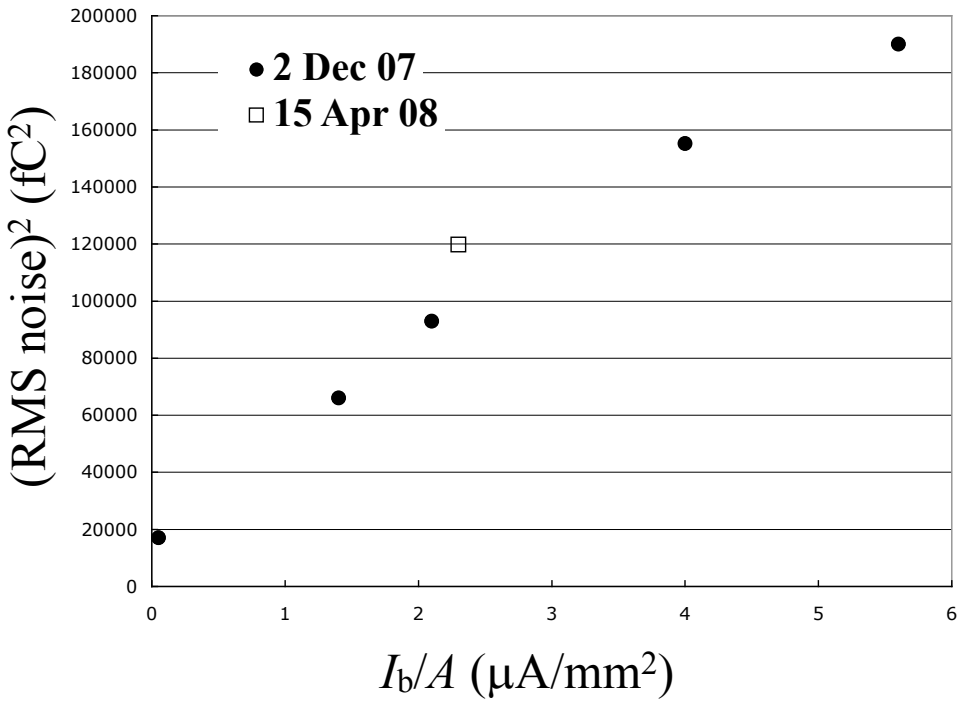

Fig. 13. Pedestal rms noise squared *vs.* leakage current for HC 1.0 mm^2 on board 2, for data taken at the time of irradiation, 2 Dec 07 (solid circles) and after room temperature annealing on 15 Apr 08 (open square).

7 FBK 1.0 mm^2

Figure 8 shows I_b as a funcion of V_b for FBK 1.0 mm^2 on board 2 for fluences of zero, 5×10^9, 10^{10}, 2×10^{10}, and 3×10^{10} protons per cm^2. The shape of the I_b *vs.* V_b distributions indicate that the gain *vs.* voltage is again relatively stable. A direct measurement of MF as a function of voltage before and after irradiation shows that the gain in the region of nominal voltage varies by about 170 fC/PE per V for FBK 1.0 mm^2 on board 1 and 110 fC/PE per V board 2. At a nominal operating voltage of $V_\mathrm{b} = 33.5$ V, the leakage current increases from 1.6 μA at zero fluence to 20.8 μA at 3×10^{10} cm^{-2}. Similar I_b *vs.* V_b curves were observed for the other FBK 1.0 mm^2 on board 1, where the leakage current at nominal voltage (33.5 V) increased from 1.6 μA at zero fluence to 6.5 μA at 10^{10} cm^{-2}.

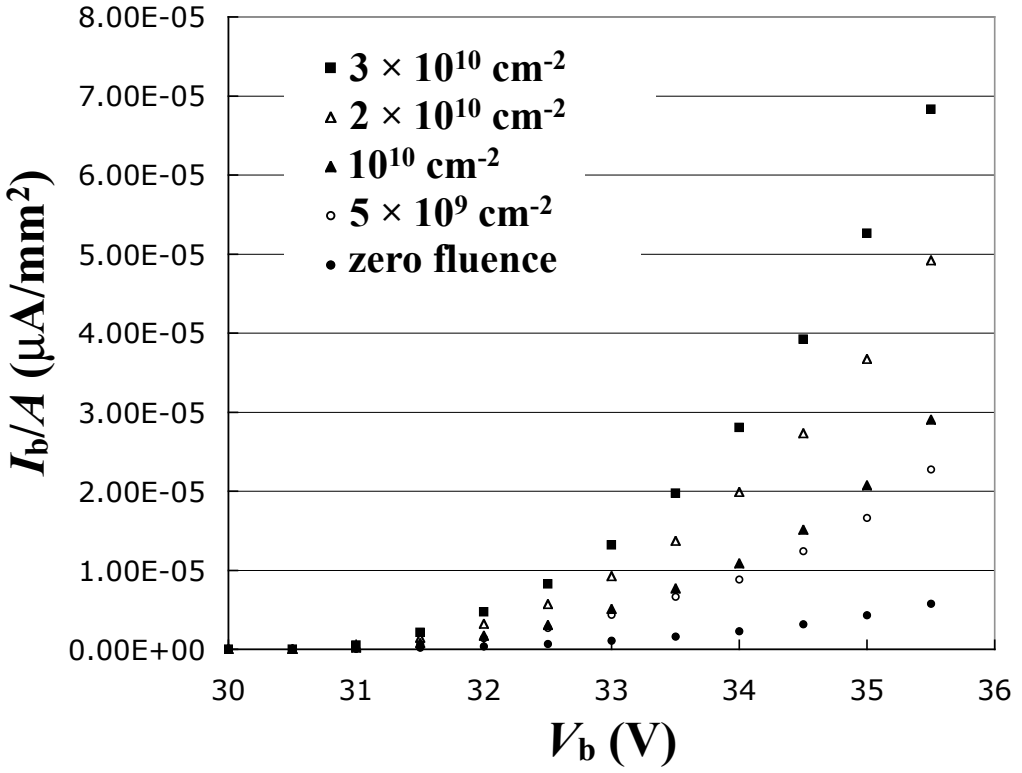

Fig. 14. Leakage currents per mm^2 for FBK 1.0 mm^2 on board 2 as a function of bias voltage for varying proton fluence.

Table 5 shows the values of I_b, MF, and n_PE/F and S/S_0. The values of n_PE are again corrected for the measured deviation of the reference diode (see Table 2). The gain times excess noise factor is observed to be stable in the range 430-450 fC/PE.

The pulse shape for 500 2 ns bins in response to the LED summed over 5000 events is shown in fig. 15 for a) zero fluence, b) 10^{10} cm^{-2}, and c) 3×10^{10} cm^{-2}

Table 5
Measured properties of the FBK 1.0 mm^2 SiPMs at V_b = 33.5 V. The data of 15Apr08 were taken after after 135 days of room temperature annealing.

Board	*Fluence* (cm^{-2})	I_b/A (μA/mm^2)	MF (fC/PE)	n_{PE}/F	S/S_0
1	zero	1.6	430	39	1
1	2.5×10^9	2.4	440	38	1.01
1	5×10^9	4.9	440	37	1.00
1	7.5×10^9	5.5	450	37	1.00
1	10^{10}	6.5	450	37	1.00
1	15Apr08	3.9	470	38	1.08
2	zero	1.6	460	35	1
2	5×10^9	5.4	460	35	0.98
2	10^{10}	7.8	480	33	0.96
2	3×10^{10}	20.8	420	37	0.89
2	15Apr08	10.7	450	33	0.92

for board 2. The pulse shape was observed to be stable at all fluences on both boards 1 and 2.

The pedestal was summed over 200 ns (bins 1-100 of fig. 15 a),b), and c)) to get the noise distributions in fC shown in fig. 15 for d) zero fluence, e) 10^{10} cm^{-2}, and f) 3×10^{10} cm^{-2} for board 2. The rms noise increases from 402 fC at zero fluence to 855 fC at 10^{10} cm^{-2} to 1367 fC at 3×10^{10} cm^{-2}. The noise distribution for FBK 1 mm^2 on board 1 was 404 fC at zero fluence, increasing to 720 fC at 10^{10} cm^{-2} for $V_b = 33.5$V.

The signal was summed over 200 ns (bins 151-250 of fig. 15 a),b), and c)) and the noise was subtracted to get the signal distributions in fC shown in fig. 15 for g) zero fluence, h) 10^{10} cm^{-2}, and i) 3×10^{10} cm^{-2} for board 2. The signal on FBK 1mm^2 on board 2, relative to zero fluence and corrected for the reference diode signal, was observed to drop by 4% at a fluence of 10^{10} cm^{-2} and 11% at 3×10^{10} cm^{-2}. The signal for FBK 1mm^2 on board 1 was observed not to change at a fluence of 10^{10} cm^{-2}.

The noise (N) distribution for FBK 1.0 mm^2 shows a clear separation for zero and single PE. Figure 16 shows the distribution of N for FBK 1.0 mm^2 on board 1 a) before irradiation, b) after a fluence of 2.5×10^9 cm^{-2}, c) after a fluence of 5×10^9 cm^{-2}, and d) after a fluence of 10^{10} cm^{-2}. Fits to the zero and single PE peaks give a gain of 370 fC/PE. Comparison of the value of MF as

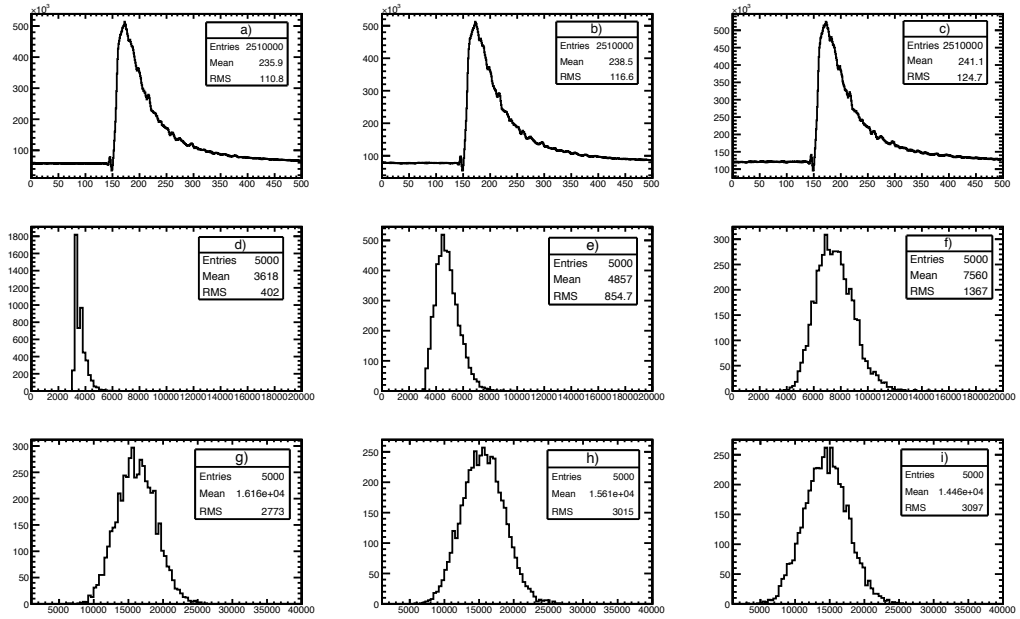

Fig. 15. FBK 1.0 mm^2 at $V_\mathrm{b} = 33.5$ V on board 2: pulse shape a) before irradiation, b) after 10^{10} cm^{-2}, and c) after 3×10^{10} cm^{-2}; noise distribution d) before irradiation, e) after 10^{10} cm^{-2}, and f) after 3×10^{10} cm^{-2}; and signal distribution in response to LED g) before irradiation, h) after 10^{10} cm^{-2}, and i) after 3×10^{10} cm^{-2}.

determined from the mean and width of the LED response (see Table 5) to the single PE peak gives $F = 1.2$, in agreement with previous measurements [1]. Locations of the zero and single PE peaks do not change with irradiation, providing additional evidence that the gain is stable. A similar single PE peak and gain is found for FBK 1.0 mm^2 on board 2.

Figure 17 shows the square of the rms noise as a function of I_b/A for FBK 1.0 mm^2 on board 2, for data taken immediately after the irradiation (2 Dec 07). The linear dependance indicates that the increase in noise is due to an increase in rate of dark counts, *i.e.* that the leakage current is proportional to the square of the number of activated pixels. On 15 Apr 08, 135 days after the irradiation, the dark current had dropped from 5.6 μA to 2.3 μA for FBK 1.0 mm^2 on board 2 and from 2.5 μA to 1.1 μA on board 1 indicating a substantial amount of annealing at room temperature. The rms of the noise distribution on 15 Apr 08 was about 2% larger than at the time of irradiation corresponding to the same leakage current as interpolated from the measurements at fluences of 10^{10} cm^{-2} and 2×10^{10} cm^{-2}.

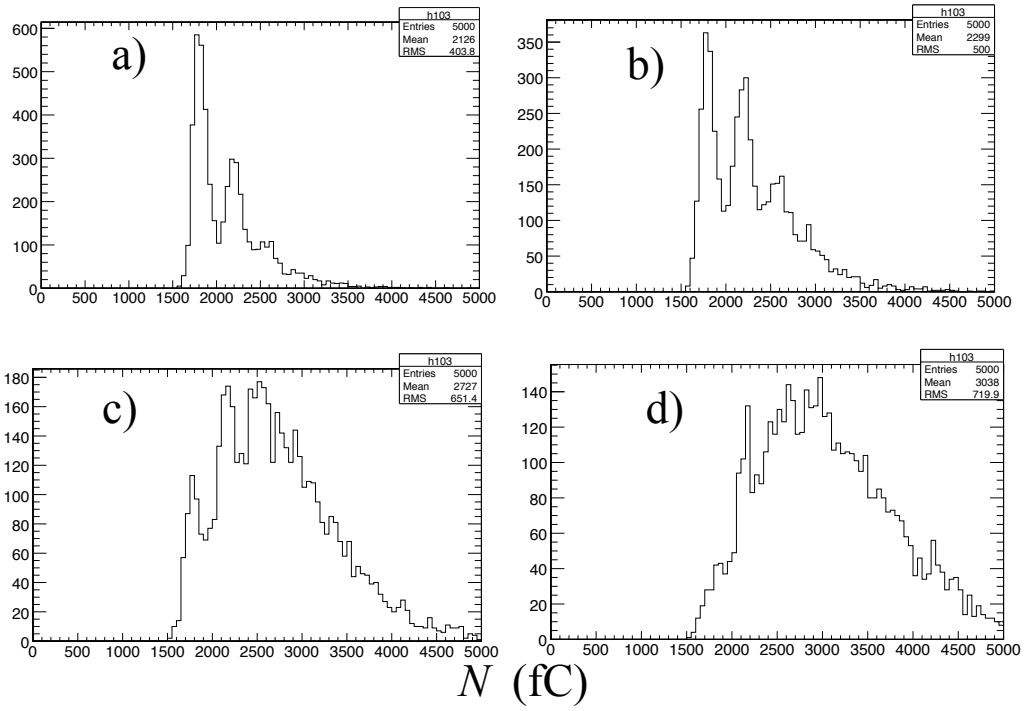

Fig. 16. Noise distribution (N) for FBK 1.0 mm^2 on board 1 a) before irradiation b) after a fluence of 2.5×10^9 cm^{-2}, c) after a fluence of 5×10^9 cm^{-2}, and d) after a fluence of 10^{10} cm^{-2}.

8 CPTA 4.4 mm^2

Figure 18 shows I_b as a function of V_b for CPTA 4.4 mm^2 on board 4 for fluences of zero, 5×10^9, 10^{10}, 2×10^{10}, and 3×10^{10} protons per cm^2. The shape of the I_b *vs.* V_b indicate that the gain *vs.* voltage is stable. A direct measurement of MF as a function of voltage before and after irradiation shows that the gain in the region of nominal voltage varies by about 19 fC/PE per V for CPTA 4.4 mm^2 on board 3 and 12 fC/PE per V for board 4. At a nominal operating voltage of $V_\mathrm{b} = 37$ V, the leakage current increases from 2.6 μA/mm^2 at zero fluence to 5.7 μA/mm^2 at 3×10^{10} cm^{-2} for board 4. Similar I_b *vs.* V_b curves were observed for the other CPTA 4.4 mm^2 on board 3, where the leakage current at nominal voltage (37 V) increased from 1.8 μA/mm^2 at zero fluence to 4.1 μA/mm^2 at 10^{10} cm^{-2}.

Table 6 shows the values of I_b, MF, and n_PE/F and S/S_0. The values of n_PE are again corrected for the measured deviation of the reference diode (see Table 2). The gain times excess noise factor is observed to decrease from 66 fC/PE to 61 fC/PE for board 1 and from 53 fC/PE to 43 fC/PE for board 2.

The pulse shape for 500 2 ns bins in response to the LED summed over 5000 events is shown in fig. 19 for a) zero fluence, b) 10^{10} cm^{-2}, and c) 3×10^{10} cm^{-2} for board 4. The pulse shape was observed to be stable at all fluences on both

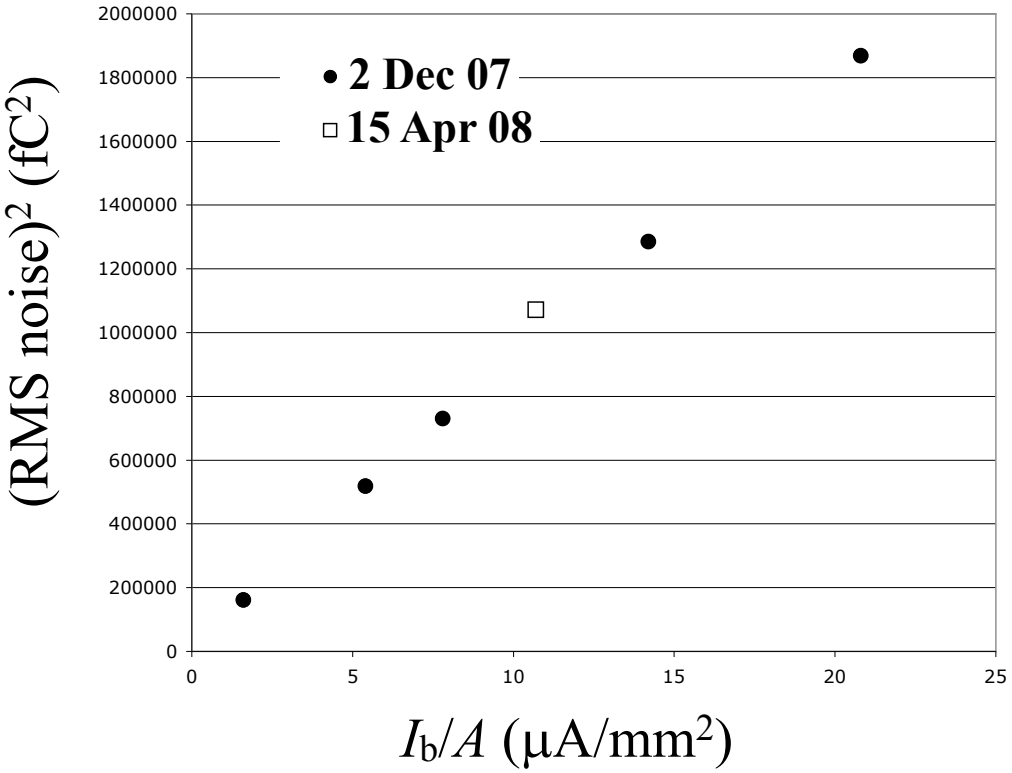

Fig. 17. Pedestal rms noise squared *vs.* leakage current for FBK 1.0 mm^2 on board 2, for data taken at the time of irradiation, 2 Dec 07 (solid circles) and after room temperature annealing on 15 Apr 08 (open square).

boards 3 and 4.

The pedestal was summed over 200 ns (bins 1-100 of fig. 19 a),b), and c)) to get the noise distributions in fC shown in fig. 19 for d) zero fluence, e) 10^{10} cm^{-2}, and f) 3×10^{10} cm^{-2} for board 4. The rms noise increases from 179 fC at zero fluence to 189 fC at 10^{10} cm^{-2} to 203 fC at 3×10^{10} cm^{-2}.

The signal was summed over 200 ns (bins 151-250 of fig. 19 a),b), and c)) and the noise was subtracted to get the signal distributions in fC shown in fig. 19 for g) zero fluence, h) 10^{10} cm^{-2}, and i) 3×10^{10} cm^{-2} for board 4. The signal on CPTA 4.4 mm^2 on board 4, relative to zero fluence and corrected for the reference diode signal, was observed to drop by 20% at a fluence of 10^{10} cm^{-2} and 49% at 3×10^{10} cm^{-2}. Similarly, the signal for CPTA 4.4 mm^2 on board 3 was 24% lower at a fluence of 10^{10} cm^{-2}. The drop in signal is due in part to a substantial drop in the number of photoelectrons (38% drop for board 4). This is due to the fact that the noise has increased to the point where a significant number of pixels are not available to respond to the LED light. This saturation is also seen in fig. 7 where the slope of the leakage current *vs.* time shows a flatttening during the last irradiation from 2×10^{10} to 3×10^{10} protons per cm^2.

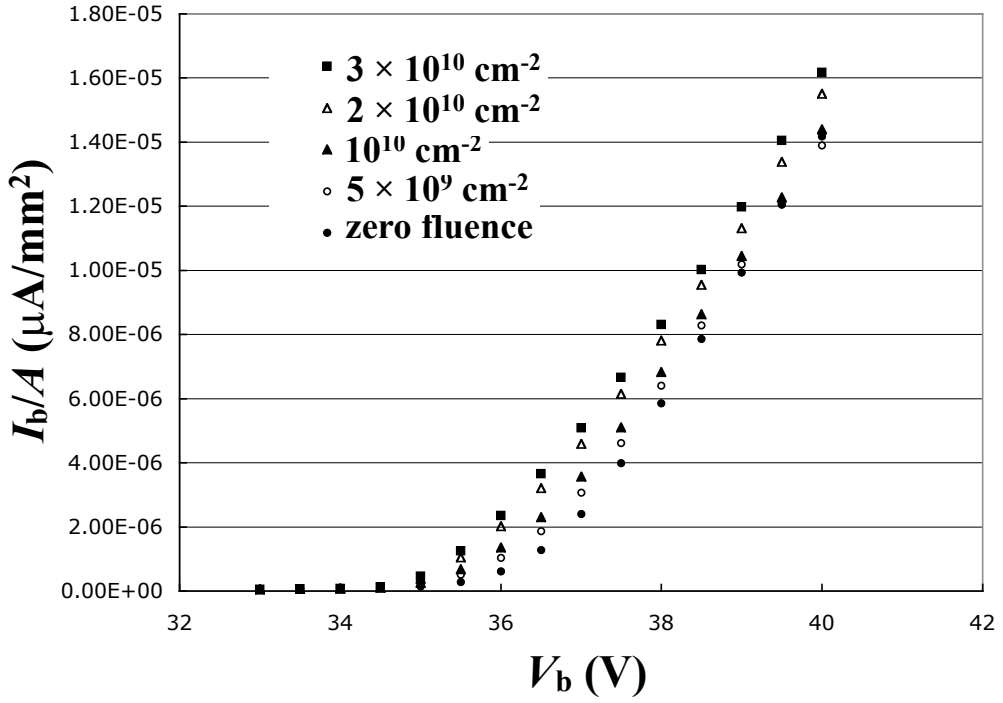

Fig. 18. Leakage currents per mm^2 for CPTA 4.4 mm^2 on board 4 as a function of bias voltage for varying proton fluence.

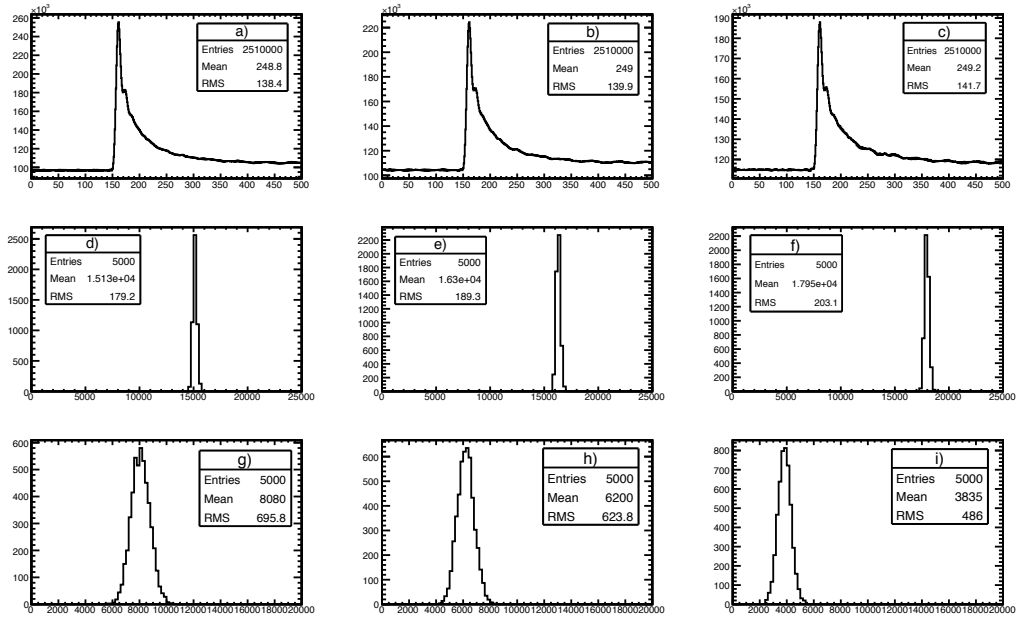

Fig. 19. CPTA 4.4 mm^2 at $V_b = 37$ V on board 4: pulse shape a) before irradiation, b) after 10^{10} cm^{-2}, and c) after 3×10^{10} cm^{-2}; noise distribution d) before irradiation, e) after 10^{10} cm^{-2}, and f) after 3×10^{10} cm^{-2}; and signal distribution in response to LED g) before irradiation, h) after 10^{10} cm^{-2}, and i) after 3×10^{10} cm^{-2}.

Table 6
Measured properties of the CPTA 4.4 mm^2 SiPMs. The bias voltage was 37 V.

Board	*Fluence* (cm^{-2})	I_b/A (μA/mm^2)	MF (fC/PE)	n_{PE}/F	S/S_0
3	zero	1.8	66	180	1
3	2.5×10^9	2.6	62	180	0.93
3	5×10^9	3.3	62	170	0.87
3	7.5×10^9	3.8	60	160	0.81
3	10^{10}	4.1	59	150	0.76
3	15Apr08	3.0	61	150	0.76
4	zero	2.6	53	152	1
4	2.5×10^9	3.0	52	145	0.93
4	5×10^9	3.4	54	133	0.89
4	7.5×10^9	3.6	51	134	0.84
4	10^{10}	3.9	52	123	0.80
4	3×10^{10}	5.7	43	95	0.51
4	15Apr08	3.9	45	102	0.57

Figure 20 shows the square of the rms noise as a function of I_b/A for CPTA 4.4 mm^2 on board 4, for data taken immediately after the irradiation (2 Dec 07). On 15 Apr 08, 135 days after the irradiation, the dark current had dropped from 5.2 μA/mm^2 to 3.6 μA/mm^2 for CPTA 4.4 mm^2 on board 4 and from 3.8 μA/mm^2 to 2.7 μA/mm^2 on board 3. The rms of the noise distribution on 15 Apr 08 was about 7% smaller than at the time of irradiation corresponding to the same leakage current at a fluence of 10^{10} cm^{-2}.

9 FBK 6.2 mm^2

Figure 21 shows I_b as a function of V_b for FBK 6.2 mm^2 on board 4 for fluences of zero, 5×10^9, 10^{10}, 2×10^{10}, and 3×10^{10} protons per cm^2. The shape of the I_b *vs.* V_b indicate that the gain *vs.* voltage is stable. A direct measurement of MF from the mean and width of the response to the LED as a function of voltage before and after irradiation shows that the gain in the region of nominal voltage varies by about 100 fC/PE per V for FK 6.2 mm^2 on boards 1 and 2. At a nominal operating voltage of $V_b = 34$ V, the leakage current increases from 0.7 μA/mm^2 at zero fluence to 9.1 μA/mm^2 at 3×10^{10} cm^{-2} for board 4. Similar I_b *vs.* V_b curves were observed for the other FBK 6.2 mm^2

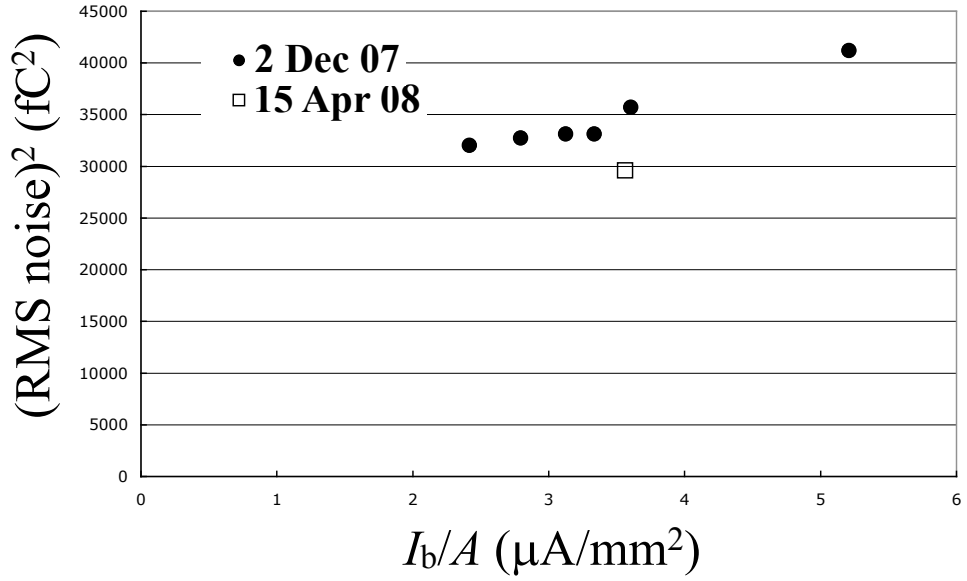

Fig. 20. Pedestal rms noise squared *vs.* I_b/A for CPTA 4.4 mm^2 on board 4, for data taken at the time of irradiation, 2 Dec 07 (solid circles) and after room temperature annealing on 15 Apr 08 (open square).

on board 3, where the leakage current at nominal voltage (34 V) increased from 1.1 μA/mm^2 at zero fluence to 5.1 μA/mm^2 at 10^{10} cm^{-2}.

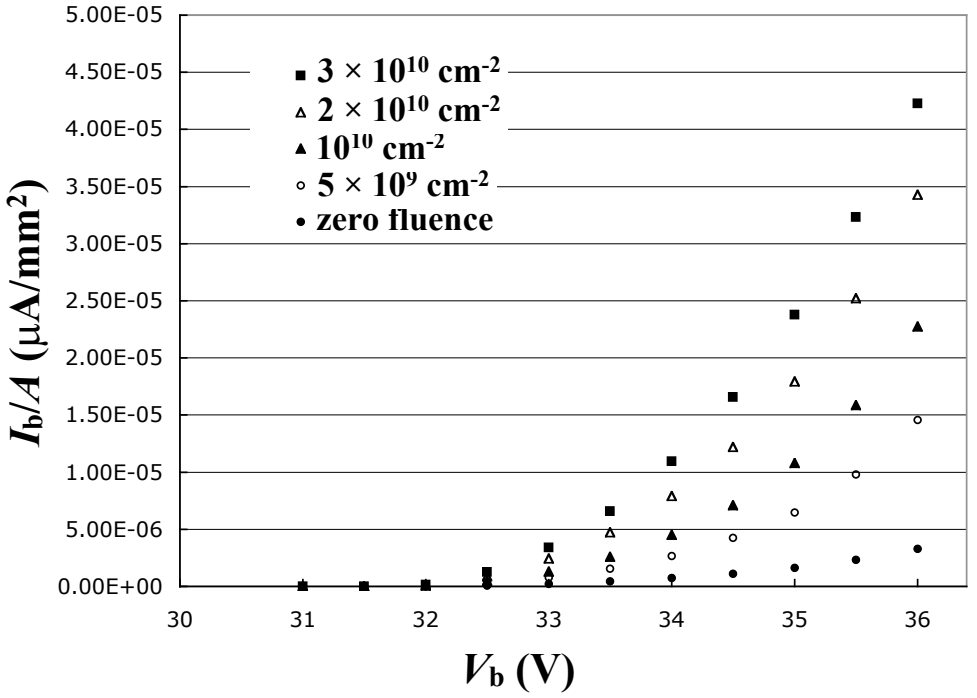

Fig. 21. Leakage currents per mm^2 for FBK 6.2 mm^2 on board 4 as a function of bias voltage for varying proton fluence.

Table 7 shows the values of I_b, MF, and n_{PE}/F and S/S_0. The values of n_{PE} are again corrected for the measured deviation of the reference diode (see Table 2). The gain times excess noise factor is observed to be stableat 200 fC/PE for board 1 and decrease from 340 fC/PE to 310 fC/PE for board 2.

Table 7
Measured properties of the FBK 6.2 mm^2 SiPMs. The bias voltage was 34 V.

Board	*Fluence* (cm^{-2})	I_b/A (μA/mm^2)	MF (fC/PE)	n_{PE}/F	S/S_0
3	zero	1.2	400	180	1
3	2.5×10^9	2.2	400	180	1.03
3	5×10^9	3.3	400	180	1.02
3	7.5×10^9	4.2	390	180	0.99
3	10^{10}	5.8	400	180	0.98
3	15Apr08	2.8	400	170	0.96
4	zero	0.8	340	170	1
4	2.5×10^9	1.7	330	170	1.00
4	5×10^9	2.6	350	160	0.99
4	7.5×10^9	3.6	330	170	0.97
4	10^{10}	4.1	320	170	0.96
4	3×10^{10}	10.1	310	150	0.84
4	15Apr08	4.9	310	170	0.93

The pulse shape for 500 2 ns bins in response to the LED summed over 5000 events is shown in fig. 22 for a) zero fluence, b) 10^{10} cm^{-2}, and c) 3×10^{10} cm^{-2} for board 4. The pulse shape was observed to be stable at all fluences on both boards 3 and 4.

The pedestal was summed over 200 ns (bins 1-100 of fig. 22 a),b), and c)) to get the noise distributions in fC shown in fig. 22 for d) zero fluence, e) 10^{10} cm^{-2}, and f) 3×10^{10} cm^{-2} for board 4. The rms noise increases from 616 fC at zero fluence to 1343 fC at 10^{10} cm^{-2} to 1984 fC at 3×10^{10} cm^{-2}.

The signal was summed over 200 ns (bins 151-250 of fig. 22 a),b), and c)) and the noise was subtracted to get the signal distributions in fC shown in fig. 22 for g) zero fluence, h) 10^{10} cm^{-2}, and i) 3×10^{10} cm^{-2} for board 4. The signal on FBK 6.2 mm^2 on board 4, relative to zero fluence and corrected for the reference diode signal, was observed to drop by 4% at a fluence of 10^{10} cm^{-2} and 16% at 3×10^{10} cm^{-2}. Similarly, the signal for FBK 6.2 mm^2 on board 3 was 2% lower at a fluence of 10^{10} cm^{-2}.

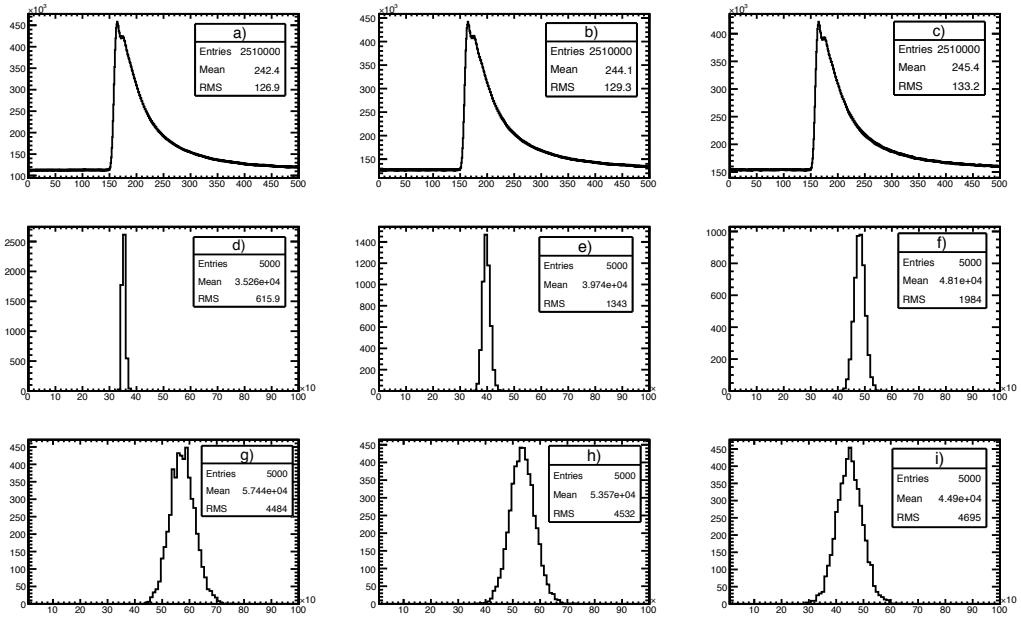

Fig. 22. FBK 6.2 mm^2 at $V_\mathrm{b} = 34$ V on board 4: pulse shape a) before irradiation, b) after 10^{10} cm^{-2}, and c) after 3×10^{10} cm^{-2}; noise distribution d) before irradiation, e) after 10^{10} cm^{-2}, and f) after 3×10^{10} cm^{-2}; and signal distribution in response to LED g) before irradiation, h) after 10^{10} cm^{-2}, and i) after 3×10^{10} cm^{-2}.

Figure 23 shows the square of the rms noise as a function of I_b/A for FBK 6.2 mm^2 on board 4, for data taken immediately after the irradiation (2 Dec 07). On 15 Apr 08, 135 days after the irradiation, the dark current had dropped from 9.1 μA/mm^2 to 4.6 μA/mm^2 for FBK 6.2 mm^2 on board 4 and from 5.1 μA/mm^2 to 2.6 μA/mm^2 on board 3. The rms of the noise distribution on 15 Apr 08 was nearly identical to the noise at the time of irradiation corresponding to the same leakage current as interpolated from the measurements at fluences of 10^{10} cm^{-2} and 2×10^{10} cm^{-2}.

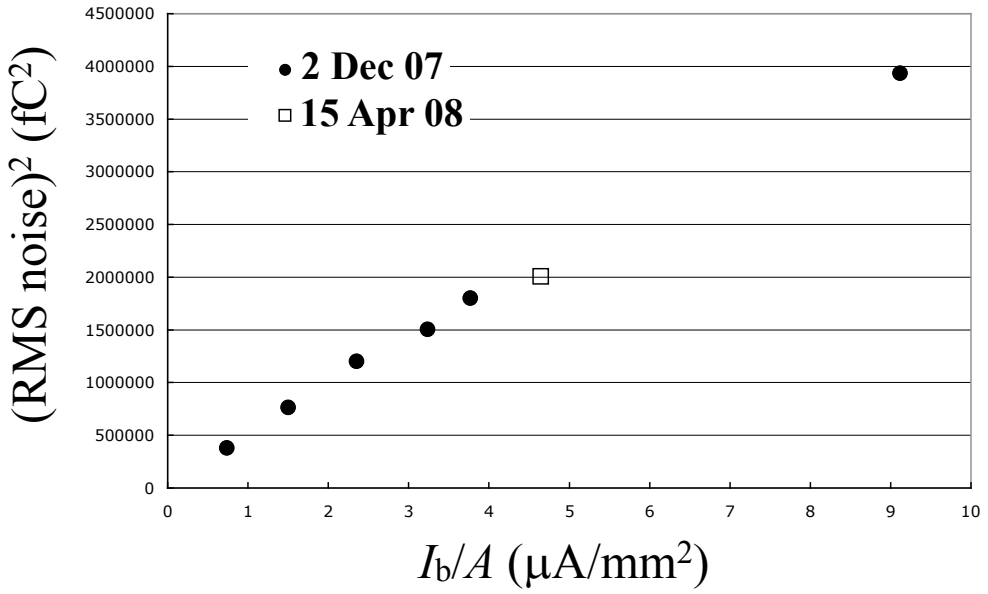

Fig. 23. Pedestal rms noise squared *vs.* I_b/A for FBK 6.2 mm^2 on board 4, for data taken at the time of irradiation, 2 Dec 07 (solid circles) and after room temperature annealing on 15 Apr 08 (open square).

10 FBK Single Pixel

Two of the FBK 6.8 mm^2 SiPMs were wired electrically to read out a single 50 μm pixel. One of these SiPMs (on board 3) developed wire bonding problems prior to the irradiation and is not discussed further. The other single pixel readout (on board 4) was operated at high gain corresponding to $V_\mathrm{b} = 37$ V to allow detection of single PEs. This SiPM was irradiated to a fluence of 3×10^{10} cm^{-2}. A total of 10k 1 μs waveforms were recorded for each partial fluence with no LED, and the pulse height was integrated over 200 ns. The resulting noise distributions are shown in fig. 24. Note the data are plotted on a log scale. The location of the single PE peak is seen at approximately 800 fC above the zero PE peak. The leakage current prior to irradiation was 22 nA. At a fluence of 3×10^{10} cm^{-2}, the leakage current had increased to 150 nA, corresponding to the same order of magnitude value of I_b/A as measured in the FBK 1.0 mm^2 and 6.2 mm^2 SiPM when extrapolated to $V_\mathrm{b} = 37$ V. The single pixel becomes slightly noisier with increasing fluence as evidenced by the single PE tail, however, the location of the single PE peak remains stable indicating the gain does not change.

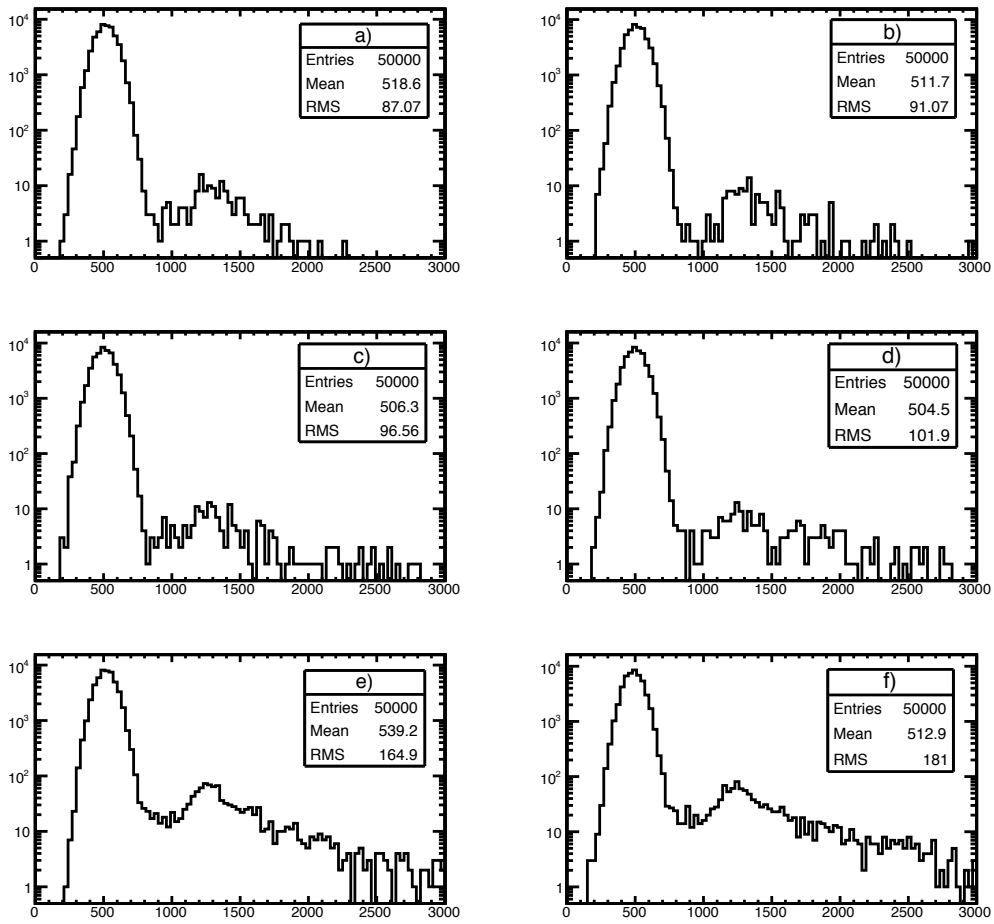

Fig. 24. Noise distribution for FBK single pixel at $V_{\rm b} = 37$ V on board 4: a) zero fluence, b) 2.5×10^9 cm^{-2}, c) 5×10^9 cm^{-2}, d) 10^{10} cm^{-2}, e) 2×10^{10} cm^{-2} and f) 3×10^{10} cm^{-2}.

11 Summary

We have exposed SiPMs manufactured by Fondazione Bruno Kessler (1 mm^2 and 6.2 mm^2), Center of Perspective Technology and Apparatus (1 mm^2 and 4.4 mm^2), and Hamamatsu Corporation (1 mm^2) using a beam of 212 MeV protons at Massachusetts General Hospital in Boston, MA. The SiPMs received fluences of up to 3×10^{10} protons per cm^2 at operating voltage. Leakage currents were read continuously during the irradiation, providing a good monitor of the condition of the SiPMs. The leakage current is found to increase in proportion to the mean square deviation of the noise distribution, indicating the dark counts are due to increased random individual pixel activation. At large values of bias currents, the gains are observed to drop due to a lowering of V_b due to the voltage drop across the 2 kΩ input resistor. There is no evidence for any increase in the excess noise factor with irradiation. Signals in response to calibrated LED pulses (fig. 25) drop by 25% for CPTA 1.0 mm^2, 15% for HC 1.0 mm^2, 4% for FBK 1.0 mm^2, 49% for CPTA 4.4 mm^2, and 16% for FBK 6.2 mm^2 SiPMs after exposure to 3×10^{10} protons per cm^{-2}. For the FBK and HC SiPMs, the reduction in signal is largely attiributed to the reduced gain under large bias currents. The larger drop for the CPTA SiPMs, especially the 4.4 mm^2 CPTA (fig. 25), can be explained by the large dead time caused by the very large quenching resistor, resulting in a μs deadtime for each pixel. In spite of the drop in signals, all of the SiPMs remained fully functional as photon counters, albeit with increased noise due to increases in dark counts. The SiPMs are found to anneal at room temperature with a reduction in the leakage current by a factor of 2 in about 100 days.

12 Acknowledgment

We acknowledge support of the U.S. National Science Foundation.

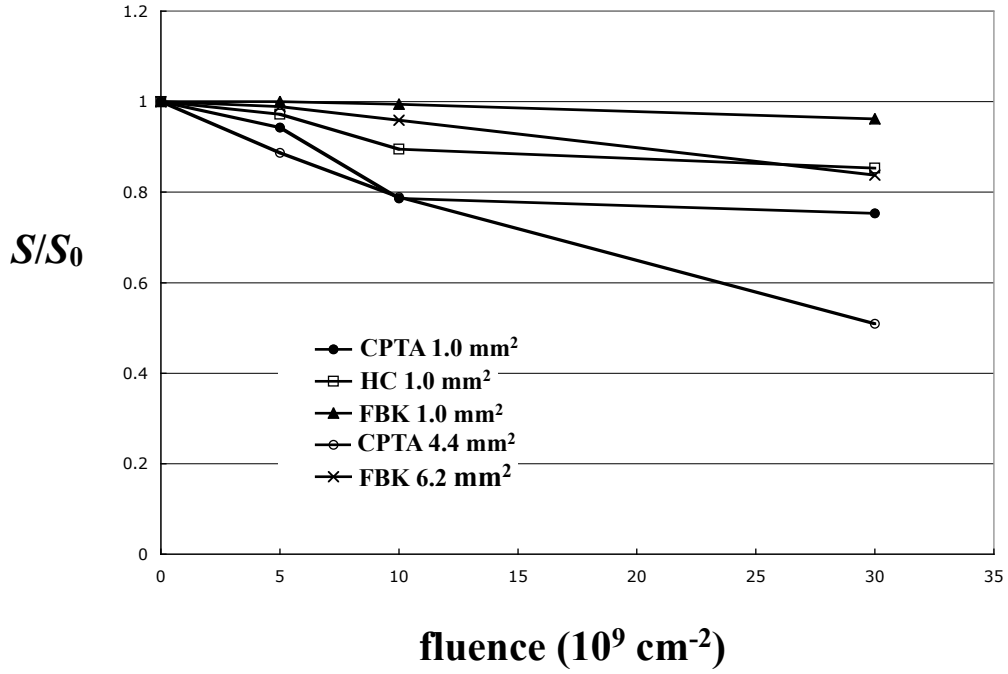

Fig. 25. Response of the SiPMs to calibrated LED pulses relative to those at zero fluence (S/S_0). The calibration of the LED pulses is done with the reference SiPMs (see Table 2).

References

[1] A. Heering *et al.*, "Performance of Silicon Photomultiplers with the CMS HCAL Front-End Electronics," Nucl. Instrum. Meth. A 576 (2007) 341.

[2] A. Heering *et al.*, "Large-Area SiPMs for the CMS Hadron Outer Calorimeter," 2007 IEEE Nuclear Science Symposium Conference Record, Vol. 2, 1545 (2007).

[3] S. Chatrchyan *et al.*, "The CMS experiment at the CERN LHC," JINST 3 (2008) S08004.

[4] "LHC Machine," Lyndon Evans and Philip Bryant (editors), JINST 3 (2008) S08001.

[5] G. Lindstrom, "Radiation Damage in Silicon Detectors," NIM A512 (2003) 30.

[6] M. Huhtinen, "Radiation Environment Simulations for the CMS Detector," CERN CMS TN/95-198.

[7] M. Huhtinen, "Optimization of the CMS forward shielding," CMS Note 2000/068.

[8] J. Rohlf, "Super-LHC: The Experimental Program," talk given at the International Workshop on Future Hadron Colliders (2003) http://conferences.fnal.gov/hadroncollider/talks/rohlf.pdf

[9] J. Freeman, "Calorimeters for the SLHC and VLHC," talk given at the International Workshop on Future Hadron Colliders (2003) http://conferences.fnal.gov/hadroncollider/talks/freeman.pdf

[10] J. Whitmore, "System Level Radiation Validation Studies for the CMS HCAL Front-End Electronics ," FERMILAB-Conf-03/316-E (2003).

[11] D. Bortoletto, "Recent Results from RD50," Nucl. Instrum. Meth. A 569 (2006) 69.

[12] E. W. Cascio *et al.*, "The Proton Irradiation Program at the Northeast Proton Therapy Center," IEEE Radiation Effects Data Workshop, 141 (2003).